Light-Induced Global Conformational Change of Photoactive Yellow Protein in Solution†

Yasushi Imamoto,* Hironari Kamikubo, Miki Harigai, Nobutaka Shimizu, and Mikio Kataoka*

Graduate School of Materials Science, Nara Institute of Science and Technology, Ikoma, Nara 630-0101, Japan

Received July 18, 2002; Revised Manuscript Received September 17, 2002

ABSTRACT: The light-induced global conformational change of photoactive yellow protein was directly observed by small-angle X-ray scattering (SAXS). The N-terminal 6, 15, or 23 amino acid residues were enzymatically truncated (T6, T15, or T23, respectively), and their near-UV intermediates were accumulated under continuous illumination for SAXS measurements. The Kratky plot demonstrated that illumination induced partial loss of globularity. The change in globularity was marked in T6 but very small in T15 and T23, suggesting that structural change in positions 7−15 mainly reduces the globularity. The radius of gyration (R_g) estimated by Guinier plot was increased by 1.1 Å for T6 and 0.7 Å for T15 and T23 upon illumination. As T23 lacks most of the N-terminal loop, structural change in the main part composed of the PAS core, helical connector, and β-scaffold caused an increase of R_g by 0.7 Å. The structural change of positions 7−15 caused an additional increase by 0.4 Å. The decrease of R_g upon truncation of positions 7−15 for dark state was 0.3 Å, while that for the intermediate was 0.7 Å, suggesting that this region moves outward on formation of the intermediate. These results indicate that a light-induced structural change of PYP takes place in the main part and N-terminal 15 amino acid residues. The former induces only dimensional increase, but the latter results in additional change in shape.

Photoactive yellow protein (PYP),[1] a photoreceptor protein found in the purple phototrophic bacterium *Ectothiorhodospira halophila* (*1*), has been proposed as a blue light receptor for negative phototaxis of the bacterium (*2*). As PYP was the first example of a photoreceptor protein responsible for light signal transduction whose tertiary structure has been characterized in high resolution, it is thought to be the most suitable target for understanding the light-capturing mechanism of living organisms at the atomic level. For this reason PYP has been extensively studied from the point of view of structural biology (*3*−*5*). PYP is composed of 125 amino acid residues and the chromophore, *trans*-*p*-coumaric acid. PYP chromophore is isomerized to the cis form upon photon absorption (*6*), and PYP undergoes a photocycle (*7*−*11*). Among the photocycle intermediates, the last one (PYP_M, also called pB or I2), whose absorption band is located in the near-UV region, is considered to be in a physiologically active form. Therefore, the structure of PYP_M needs to be clarified and compared with that of the dark state in order to understand the activation mechanism of photoexcited PYP.

The absorption maximum of PYP_M is blue shifted because the phenolic oxygen of the chromophore is donated a proton by Glu46 (*12*). The structure of PYP_M has been analyzed by time-resolved crystallography (*13*), demonstrating that the amino acid residues near the chromophore are rearranged and Arg52 is exposed to the solvent upon formation of PYP_M. We recently probed the surface charge of PYP_M in solution by using multivalent organic acids such as citrate and demonstrated that citrate specifically binds to PYP_M (*14*). This suggests that the positive charge is exposed to the solvent upon formation of PYP_M in solution, which is consistent with the model proposed by crystallography. However, although the structural difference between PYP and PYP_M in the crystal is limited to the region around the chromophore, accumulated evidence strongly suggests that the structural change under physiological conditions is much larger than that in the crystal, probably because conformational change is restricted in the crystal.

Much spectroscopic data for PYP_M in solution have been accumulated to date. Comparison of far-UV circular dichroism spectra of PYP and PYP_M demonstrated that the contents of the α-helix and/or β-sheet are decreased upon conversion from PYP to PYP_M (*15*, *16*). The difference Fourier transform infrared spectrum between PYP and PYP_M recorded in solution shows much a larger absorbance change in the amide mode region (*17*, *18*) than in the crystal, suggesting that the backbone structure is largely altered in solution, unlike in the crystal. Some of the structural information for dark state PYP provided by NMR was lost for PYP_M (*19*), suggesting extensive structural disorder. The study of the photoreaction of PYP in the presence of urea demonstrated that PYP_M is less stabile against denaturants than PYP (*20*). Transient spectroscopy with a millisecond time scale using site-directed mutants of PYP suggested that the chromophore/protein

† This work was supported in part by a Grant-in-Aid for Scientific Research from the Ministry of Education, Culture, Sports, Science, and Technology of Japan.

* To whom correspondence should be addressed. Y.I.: phone, +81-743-72-6101; fax, +81-743-72-6109; e-mail, imamoto@ms.aist-nara.ac.jp. M.K.: phone, +81-743-72-6100; fax, +81-743-72-6109; e-mail, kataoka@ms.aist-nara.ac.jp.

[1] Abbreviations: PYP, photoactive yellow protein from *Ectothiorhodospira halophila*; T*n*, PYP which lacks N-terminal *n* amino acid residues; MOPS, 3-(*N*-morpholino)propanesulfonic acid; FTIR, Fourier transform infrared; SAXS, small-angle X-ray scattering; R_g, radius of gyration.

10.1021/bi0264768 CCC: $22.00
Published on Web 10/24/2002

interaction of PYP_M in solution is quite different from that in the crystal (*21*). Finally, recent SAXS measurement using the M100L mutant (*16*) or under acidic conditions (*14*) demonstrated that R_g of PYP is significantly increased upon formation of PYP_M. This accumulated evidence strongly suggests that the structure of PYP_M is strikingly different from that of PYP in the dark, and PYP_M assumes a partially unfolded structure. However, what kind of structural change takes place has not been substantially elucidated.

The main reason why detailed characterization of PYP_M is difficult is its short lifetime (about 100 ms under physiological conditions). Hence in the previous studies, PYP_M was stabilized by acidification or site-directed mutagenesis around the chromophore. We have developed alternative methods to stabilize PYP_M by enzymatic truncation of the N-terminal region (*22*).

We have reported that bovine pancreas chymotrypsin selectively cleaves the peptide bonds at positions 6−7, 15−16, and 23−24 (*22*). The truncated PYP, which lacks the N-terminal 6, 15, or 23 amino acid residues (T6, T15, or T23, respectively), can be isolated from the reaction mixture by DEAE-Sepharose column chromatography. The lifetimes of M intermediates from T6, T15, and T23 ($T6_M$, $T15_M$ and $T23_M$, respectively) at pH 7.0, 20 °C, are 18, 300, and 600 s, respectively, whereas that of intact PYP_M was 130 ms (*22*).

Utilization of truncated PYPs has several advantages. First, measurements can be made under physiological conditions. Enough PYP_M can be accumulated under photo steady state produced by continuous illumination at neutral pH and an ordinary temperature. Second, because the N-terminal loop and chromophore binding site are located on opposite sides of the β-sheet, the chromophore binding site is not affected by cleaving the N-terminal region (*22*). Site-directed mutants which have markedly long-lived PYP_M have mutations near the chromophore (for example, M100L and R52Q), in which hydrogen-bonding network around the chromophore may be altered. In addition, systematic analysis using T6, T15, and T23 may give site-specific information on structural change that occurs in the N-terminal region.

In the present study, light-induced structural change was studied by small-angle X-ray scattering (SAXS) using truncated PYPs. The radius of gyration (R_g) was estimated by a Guinier plot of SAXS pattern, and globularity was examined by a Kratky plot. On the basis of these results, light-induced conformational change of PYP is discussed.

MATERIALS AND METHODS

Sample Preparation. PYP of *E. halophila* was heterologously overexpressed by *Escherichia coli*, reconstituted by adding *p*-coumaric anhydride, and purified by DEAE-Sepharose (Amersham Biosciences, Piscataway, NJ) column chromatography as reported previously (*23*, *24*). The N-terminal 6, 15, or 23 amino acid residues of PYP were truncated by bovine pancreas chymotrypsin (*22*). Truncated PYPs (T6, T15, and T23) in the reaction mixture were separated by DEAE-Sepharose column chromatography (*22*). Finally, PYPs were suspended in MOPS buffer (10 mM MOPS, 200 mM NaCl, pH 7.0) at concentrations of 2−12 mg/mL.

UV−Visible Spectroscopy. UV−visible spectra were recorded with a multichannel CCD/fiber optic spectroscopy system (S2000 system; Ocean Optics, Dunedin, FL). The sample was illuminated by a 100 W optical fiber illuminator (Megalight 100; Hoya-Schott, Tokyo, Japan) equipped with a glass optical filter (Y43; Asahi Techno Glass, Chiba, Japan), which transmits >410 nm light. The absorption spectra of the samples (1 mm light path length) were measured in the dark and under continuous illumination with >410 nm light. The temperature of the sample was kept at 20 °C.

SAXS Measurements. SAXS measurements were carried out at Beam Line BL10C in the Photon Factory of the High Energy Accelerator Research Organization (Tsukuba, Japan). Eighty microliters of the sample was placed in the sample cell (1 mm light path length), and the scattering patterns were measured with a PSPC (position-sensitive proportional counter) (*25*).

In the small angle region, the scattering intensity at Q [$I(Q)$] is expressed as

$$I(Q) \cong I(0) \exp(-{}^1/_3 Q^2 R_g{}^2) \quad (1)$$

where $Q = 4\pi \sin \theta/\lambda$ is the amplitude of the scattering vector, 2θ is the scattering angle, λ is the wavelength of the X-ray (1.488 Å), $I(0)$ is the scattering intensity at $Q = 0$, and R_g is the radius of gyration. The slope and Y-intersection of a Guinier plot [ln $I(Q)$ vs Q^2] give ln $I(0)$ and $R_g{}^2$, respectively. The shapes of PYPs and intermediates were examined by Kratky plot after normalizing the molecular weight and dimensions using $I(0)$ and R_g [$Q^2 R_g{}^2 I(Q)/I(0)$ vs QR_g]. The scattering patterns for the dark state and photo steady state were measured in the dark and under continuous illumination with >410 nm light. The temperature of the sample was kept at 20 °C.

Calculation of the Scattering Profile from the Crystal Structure. SAXS profiles of PYP and PYP_M (I2) in the crystal were calculated using CRYSOL software (*26*) by setting the hydration shell width at 3 Å. For intact PYP, the SAXS profile was calculated using PDB ID 2PHY, while for T6, T15, and T23 profiles were similarly calculated after the coordinates for the N-terminal 6, 15, and 23 amino acid residues were deleted from 2PHY. For PYP_M, PDB ID 2PYP was used. R_g in the crystal was estimated from the Guinier plot of these profiles.

RESULTS

The limited lifetime of PYP_M prevents detailed characterization of PYP_M by SAXS. To overcome this difficulty, PYP_M was stabilized by truncation of several N-terminal amino acid residues. The amount of PYP_M in the photo steady state was first estimated by UV−visible spectroscopy (Figure 1).

The absorption spectra of intact PYP, T6, T15, and T23 (pH 7.0, 293 K) were measured in the dark. The absorption maxima were located at 445 nm for T6, 443 nm for T15, and 442 nm for T23, whereas for intact PYP it was 446 nm. Then the absorption spectra of the photo-steady-state mixture produced by >410 nm were recorded. Illumination decreased the absorbance at 446 nm but increased it at 360 nm, indicating that the photo-steady-state mixture was composed of the dark state and M intermediate. However, the decrease of the dark state varied according to the lifetime of the respective M intermediate. About 3% of intact PYP was

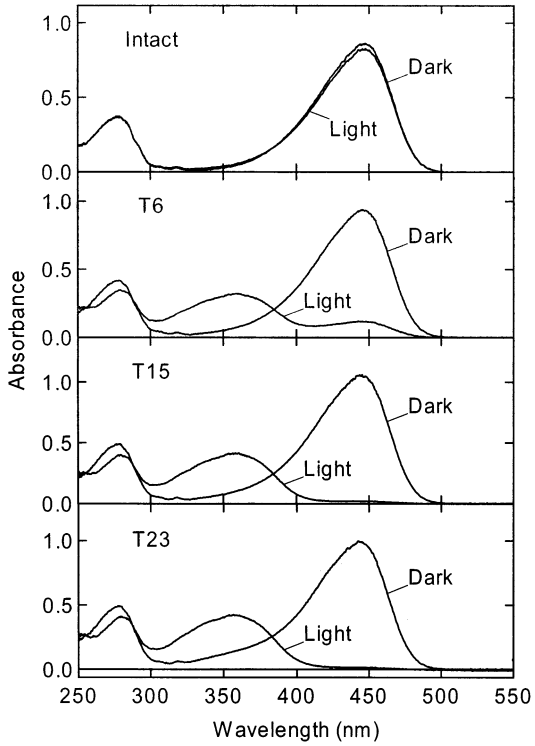

FIGURE 1: Accumulation of M intermediates from intact PYP, T6, T15, and T23. The sample (~4 mg/mL) was placed in a sample cell of 1 mm light path length. The absorption spectrum of the sample was recorded in the dark (Dark) and under continuous illumination with >410 nm light (Light).

converted to PYP_M under the present irradiation conditions. However, about 90% of T6 and almost all T15 and T23 were converted to their M intermediates ($T6_M$, $T15_M$, and $T23_M$, respectively). The absorption maxima of the photo-steady-state mixtures produced from T6, T15, and T23 were all 357 nm, which is in good agreement with the absorption maximum of intact PYP_M (*21*).

To examine the reversibility of this photoconversion, the difference FTIR spectra between light and dark conditions (PYP_M minus PYP) were repeatedly measured in the same irradiation condition (data not shown). The results demonstrated that the difference FTIR spectra were reproducibly obtained for all PYPs. In addition, the spectra were not altered by changing the intensity of the excitation light. Because FTIR spectroscopy is sensitive to the changes in the protein backbone as well as the chromophore, these observations indicate that the artifactual structural change caused by intense prolonged light did not take place.

SAXS measurements were carried out under the same conditions. The scattering patterns of dark states were measured, and then the scattering patterns of photo steady states were measured under continuous illumination with >410 nm light. In Figure 2, the logarithms of scattering intensities at various concentrations were plotted against Q^2 (Guinier plots).

It is well established that the Guinier plot is linear in $QR_g < 1$ regardless of the shape of the scatterer. However, the linear region for the globular protein sometimes expands to $QR_g < 2$ (*27*). In fact, our previous SAXS experiment (*14*) has demonstrated that the linear regions for intact PYP and PYP_M in the acidic condition are $Q^2 < 0.02$ Å^{-2} ($QR_g < 2$). Because the R_g values roughly estimated from the present

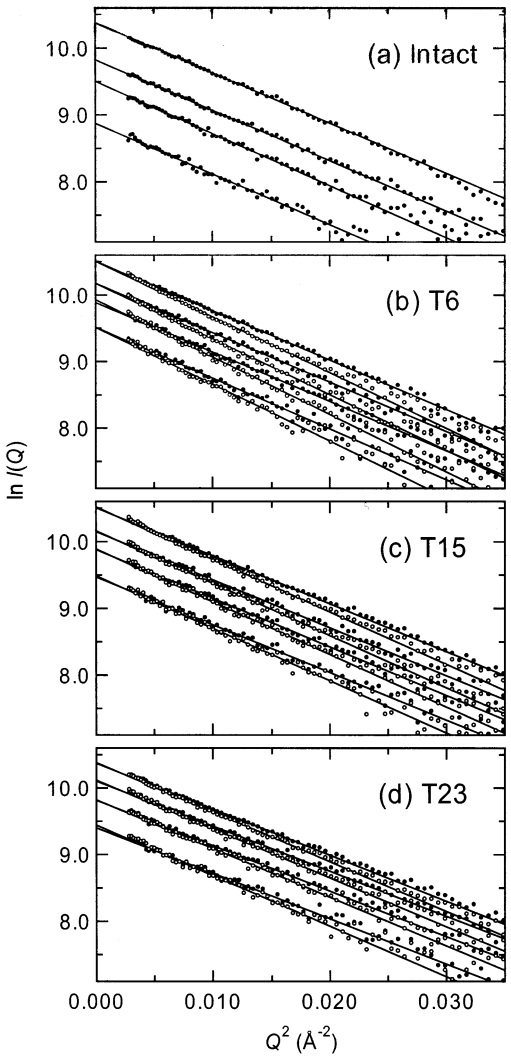

FIGURE 2: Guinier plots of intact PYP, T6, T15, and T23. SAXS patterns were measured in the dark (closed circles) and under continuous illumination with >410 nm light (open circles). Each trace was fitted by a linear line in $Q^2 < 0.02$ Å^{-2}. (a) Intact PYP at concentrations of 10, 6, 4, and 2 mg/mL (from top to bottom). (b) T6 at concentrations of 12, 8, 6, and 4 mg/mL (from top to bottom). (c) T15 at concentrations of 12, 8, 6, and 4 mg/mL (from top to bottom). (d) T23 at concentrations of 10, 8, 6, and 4 mg/mL (from top to bottom).

data were comparable to previous ones, each trace was fitted by a linear line in $Q^2 < 0.02$ Å^{-2}.

R_g^2 and $I(0)$ were estimated from the slope and *Y*-intersection of the Guinier plot, respectively. The slope for the illuminated condition was steeper than that in the dark, indicating an increase of R_g^2 by light. However, no significant difference in the *Y*-intersection was observed between dark and light conditions for each sample. As $I(0)$ divided by weight concentration [$I(0)$/conc] is proportional to the molecular weight of the scatterer, this indicates that no aggregation was induced by light. Therefore, the increase of R_g^2 is attributable to conformational change of a single PYP molecule.

$I(0)$/conc and R_g are possibly dependent on protein concentration because of interparticle interaction. Hence the intrinsic values for $I(0)$/conc and R_g^2 should be estimated at sufficiently low protein concentrations. $I(0)$/conc values for the dark state PYP, T6, T15, and T23 measured at various

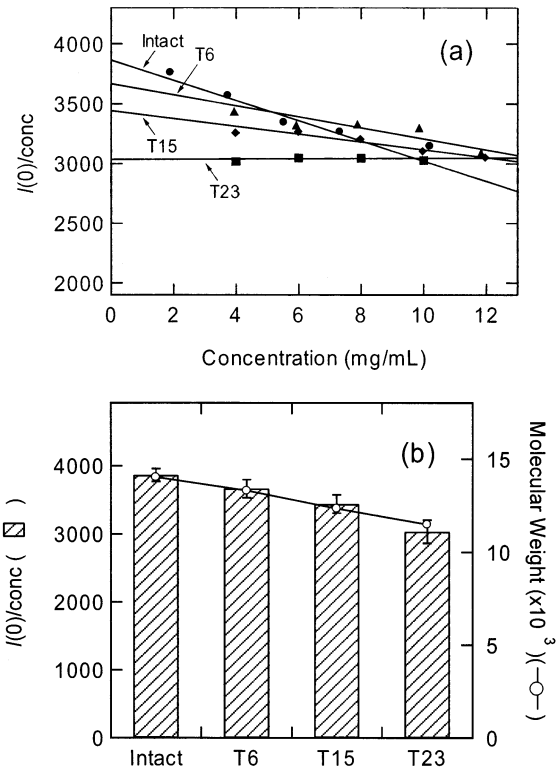

FIGURE 3: Concentration dependence of $I(0)$/conc. (a) $I(0)$/conc for intact PYP (circles), T6 (triangles), T15 (diamonds), and T23 (squares) in the dark plotted against concentration. They were fit to linear lines, and the intrinsic $I(0)$/conc was estimated by Y-intersection. (b) The plot of $I(0)$/conc was superimposed on the plot of molecular weight.

Table 1: $I(0)$ and R_g of PYPs and Intermediates

			R_g (Å)	
	mol wt	$I(0)$/conc	calcd[a]	exptl[b]
intact	14019.8	3860 ± 90	15.4	15.2 ± 0.2
T6	13305.0	3670 ± 130	15.1	15.0 ± 0.2
$T6_M$				16.1 ± 0.2
T15	12346.0	3440 ± 130	14.8	14.7 ± 0.2
$T15_M$				15.4 ± 0.2
T23	11487.0	3040 ± 170	14.3	14.1 ± 0.2
$T23_M$				14.8 ± 0.2

[a] Calculated from PDB ID 2PHY. [b] Experimentally determined.

concentrations were plotted against concentration and fitted by linear lines (Figure 3a). The slope of the line became gentler as the number of truncated amino acid residues increased, indicating that interparticle interaction is altered due to changes in surface properties. The intrinsic $I(0)$/conc was then estimated by the Y-intersection (Table 1). The plots of molecular weights calculated from the amino acid sequences of intact and truncated PYPs were superimposed on the plot of $I(0)$/conc (Figure 3b). They were consistent with each other, indicating that no aggregations are present in the sample, and the values obtained by the present experiments are attributable to the monodispersed molecules.

R_g^2 for intact PYP in the dark and for T6, T15, and T23 in the dark and under illumination were then plotted against concentration (Figure 4). They were fitted by linear lines, and the intrinsic R_g^2 was estimated by Y-intersection (Table 1 and Figure 4e). R_g values for the dark states were slightly decreased by truncation (Table 1). The experimentally

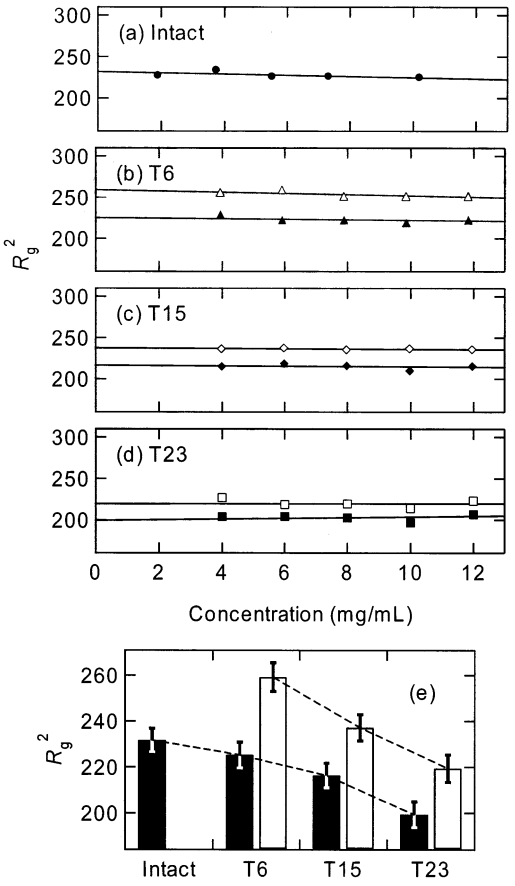

FIGURE 4: Concentration dependence of R_g^2. R_g^2 in the dark (closed symbols) and with >410 nm light (open symbols) was plotted against the concentration. They were fit to linear lines, and intrinsic R_g^2 was estimated by Y-intersection. (a) Intact PYP, (b) T6, (c) T15, (d) T23, (e) comparison of R_g^2 in the dark (black) and with light (white).

obtained R_g values were compared with those calculated from the crystal structure (Table 1). The scattering profile for the crystal structure was calculated by CRYSOL software (*26*) using the coordinates of 2PHY. Scattering profiles for T6, T15, and T23 in the crystal were calculated after the coordinates for 6, 15, and 23 amino acids were deleted from 2PHY. These scattering profiles were Guinier plotted, and R_g^2 was estimated by fitting a linear line in Q^2 ranging from 0 to 0.02 $Å^{-2}$. R_g was calculated to be 15.4 Å for intact PYP, 15.1 Å for T6, 14.8 Å for T15, and 14.3 Å for T23. Although the calculated values were 0.1−0.2 Å greater than the experimental ones, the decreases in R_g by truncation agreed well with each other.

Upon illumination, R_g^2 values of truncated PYPs were markedly increased, while $I(0)$ values were unchanged (Figure 2). R_g^2 under illumination was plotted against concentration, and intrinsic values were similarly estimated by Y-intersection (Table 1). The increase in R_g by illumination was 1.1 Å for T6 and 0.7 Å for T15 and T23.

Changes in shapes of PYP molecules by light were examined by Kratky plot (Figure 5). The molecular weight is decreased by truncation, and the dimension (R_g) is increased by light (Table 1). These changes cause a reduction in peak height of the Kratky plot [$Q^2I(Q)$ vs Q] even if globularity is maintained. Hence the molecular weight and dimension were normalized by plotting $Q^2R_g^2I(Q)/I(0)$ against QR_g. The Kratky plots for intact and truncated PYPs in the

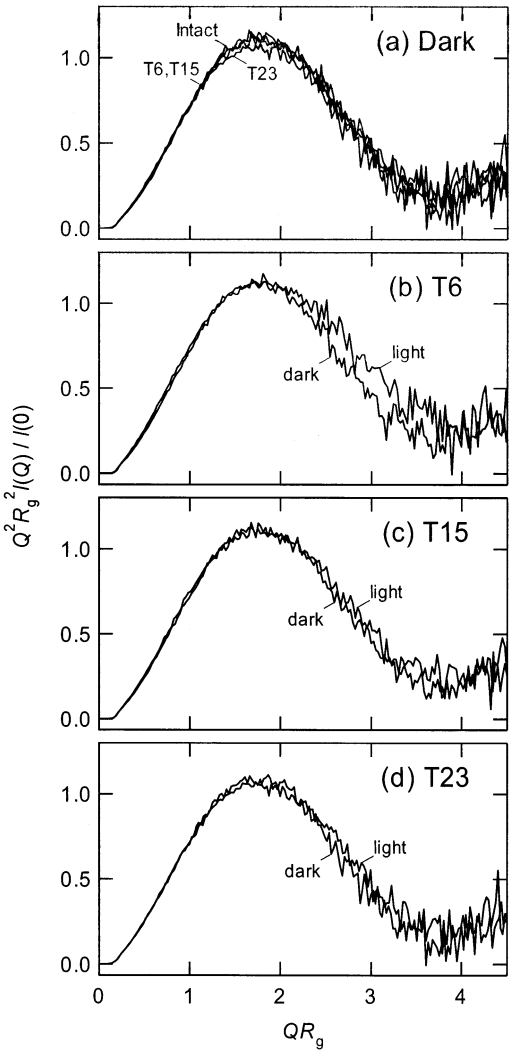

FIGURE 5: Normalized Kratky plots of truncated PYPs and intermediates. (a) The plots of intact PYP, T6, T15, and T23 in the dark compared to each other. (b−d) The plots of T6, T15, and T23 in the dark compared with those under continuous illumination.

dark show clear peaks at $QR_g = 1.8$, indicating that they are in globular structures. As they overlapped within experimental error (Figure 5a), the truncated PYPs have globularity comparable to that of intact PYP. These patterns also agreed with the scattering patterns calculated by CRYSOL (not shown), confirming that truncation of the N-terminal region does not induce a large structural change in the residual part. From illumination, the shapes from $QR_g = 0-1.8$ did not change, but the traces went upward for $QR_g > 1.8$. The change in T6 was clear, but those in T15 and T23 were almost into the noise. The increase in bandwidth indicates partial loss of globularity upon the formation of $T6_M$. We have recorded the SAXS profile of intact PYP_M under acidic conditions (*14*), in which the change in normalized Kratky plot by light was larger than T15 and T23 and comparable to T6 (not shown). As T23 lacks most of the N-terminal loop, the Kratky plots of T23 and $T23_M$ represent the shape of the main part, composed of the PAS core, helical connector, and β-scaffold (*28*), of PYP and PYP_M. No significant change in the Kratky plot of T23 therefore suggests that structural change in the main part of PYP results in no change in shape, although its dimensions are increased by 0.7 Å. These results strongly suggest that partial loss of globularity from illumination is due to structural change of the N-terminal 15 amino acid residues.

DISCUSSION

Spectroscopic data accumulated to date suggest that PYP_M in solution assumes a strikingly different structure from dark state PYP, unlike in the crystal. It has been suggested that PYP_M is in a partially unfolded structure, but what kind of structural change takes place has not been substantially demonstrated. Due to the limited lifetime of PYP_M, its characterization has been difficult. In the present study, PYP_M was stabilized by enzymatic truncation of the N-terminal region (*22*). As the chromophore binding site and N-terminus are located on opposite sides of the β-sheet, the effect of truncation on the chromophore binding site is expected to be small. In fact, the absorption spectra of $T6_M$, $T15_M$, and $T23_M$ are identical to that of PYP_M (*22*), suggesting that the chromophore/protein interaction in PYP_M is not altered by truncation.

SAXS experiments clearly demonstrated an increase in R_g upon illumination of truncated PYPs. Despite the increase of R_g, $I(0)$ was not significantly changed by irradiation (Figure 2). In addition, $I(0)$/conc of intact and truncated PYPs experimentally obtained here were consistent with their molecular weights (Figure 3). Together, the differences in R_g observed in the present experiments are attributable not to aggregation states but to the structures of the monodispersed PYP molecule. Therefore, these results confirm that global conformational change on formation of M intermediate also takes place under physiological conditions, without modification of the chromophore binding site.

Estimation of R_g by CRYSOL using the crystal structure suggested that truncation of 6, 15, or 23 amino acid residues results in a decrease of R_g by 0.3, 0.6, or 1.1 Å, respectively, which agreed with the present data (Table 1). In addition, the scattering pattern calculated by CRYSOL reproduced the Kratky plots of intact and truncated PYPs in the dark very well (not shown). These observations strongly suggest that truncation of the N-terminal region does not affect the structure of the residual part in the dark state. However, the slope of $I(0)$/conc vs concentration for intact PYP was steeper than for T6, T15, and T23 (Figure 3a). This indicates that interparticle interaction of intact PYP is different from that for truncated forms, and thus surface properties are changed by removal of the N-terminal region. The N-terminal loop is rich in acidic amino acid residues. In addition, hydrophobic side chains are located between the β-sheet and N-terminal loop. Thus the decrease in electrostatic repulsion and/or the increase in hydrophobic interaction by truncation is likely to weaken interparticle interaction.

While the present SAXS experiment clearly demonstrated the light-induced increase of R_g, the difference in R_g between PYP_M and the dark state in the crystal, calculated using 2PYP, was ~0.01 Å, indicating that the structural change in the crystal is too small to be detected by SAXS experiments. The structural change in solution is thus much larger than that in the crystal. It should be noted that the increase of R_g observed in the T6 → $T6_M$ transition (1.1 Å) is comparable to the decrease of R_g by removal of 23 amino acid residues from the dark state PYP.

Truncation of the N-terminal region alters light-induced R_g increase as well as the lifetime of PYP_M. This strongly

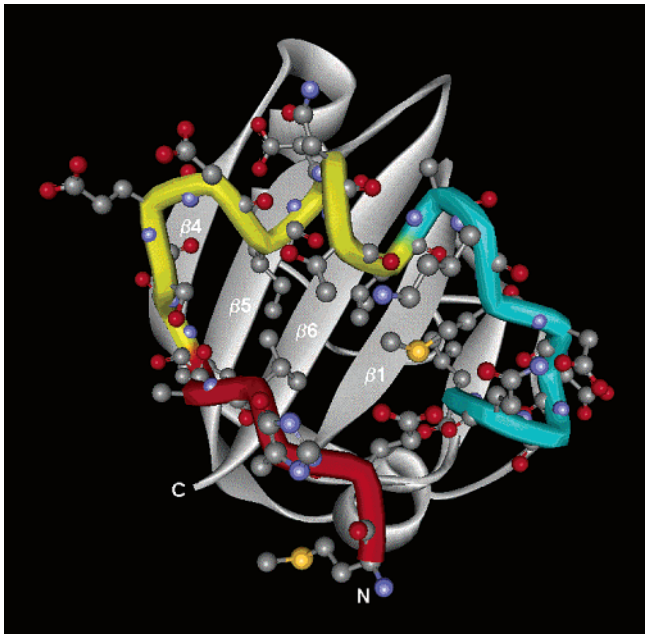

FIGURE 6: Structure of the N-terminal loop in the dark (PDB ID 2PHY). Positions 1−6, 7−15, and 16−23 are colored in red, yellow, and blue, respectively. The present experiment suggests that the residues from Gly7 to Leu15 are detached from the β-sheet upon formation of PYP_M.

suggests that the N-terminal region is important for formation and decay of PYP_M. The crystal structure shows that the N-terminal region, which incorporates two short α-helices, forms a ring in the dark (Figure 6). This ring lies parallel to the plane of the β-sheet. It is closed by a hydrogen bond between the amide nitrogen of Glu2 and the amide oxygen of Gly25. Amino acid residues from Met1 to Phe6 have the greatest effect on decay of PYP_M: truncation of this region results in a 140-fold longer lifetime. In T6, the hydrogen bond between Glu2 and Gly25 is lacking and the N-terminal loop is open, which is likely to greatly prolong the lifetime of PYP_M.

It should be noted that the difference in R_g between T6 and T15 was 0.3 Å, but that between $T6_M$ and $T15_M$ was 0.7 Å (Table 1). In contrast, the difference in R_g between T15 and T23 was 0.6 Å for both dark and light conditions. Namely, the decrease of R_g by removal of Gly7−Leu15 in the M state was larger than that in the dark state, but that of Ala16−Leu23 was constant. This suggests that Gly7−Leu15 has a more important role in structural change of PYP than Ala16−Leu23.

The most simple and straightforward explanation for the difference in decrease of R_g between T6 → T15 and $T6_M$ → $T15_M$ would be that residues from Gly7 to Leu15 in $T6_M$ are more responsible for R_g than T6. R_g^2 is expressed as

$$R_g^2 = \frac{\int_V \rho(r) r^2 \, dV}{\int_V \rho(r) \, dV}$$

where r is the location vector, $\rho(r)$ is the electron density at r, and V is the volume. The denominator is the total amount of electrons, and it is not changed by light. Assuming that the movement of the center of gravity of the electron upon truncation is negligible, the change in R_g^2 by truncation is mainly due to r^2, the square of the distance from the center. This means that Gly7−Leu15 in the dark state is located more proximately to the center than in the M intermediate.

The Kratky plot also suggests conformational change in residues from Gly7 to Leu15. The light-induced changes in globularity for T15 and T23 were almost negligible, while for T6 it was marked. The change for T6 was comparable to that for the intact PYP under acidic conditions (not shown), suggesting that partial loss of globularity from illumination is due to structural change of these residues.

This explanation is based on the premise that the light-induced structural changes in T6, T15, and T23 reflect that in intact PYP. Here we should discuss the possibility that the enzymatic truncation of the N-terminal region alters the light-induced structural change of PYP. Namely, N-terminal region may enhance the structural change of the main part composed of the PAS core, helical connector, and β-scaffold, resulting in larger structural change in T6 → $T6_M$ than that in T15 → $T15_M$ and T23 → $T23_M$. Alternatively, truncation may destabilize the native PYP structure, and the creation of the light-generated PYP_M state further destabilizes the native fold, causing larger global structural change in the truncated PYPs than in the intact PYP. Because R_g values of intact PYP, T6, T15, and T23 in the dark states obtained by SAXS experiments agree with those calculated from the crystal structure, the disorder of the structure in the dark states by truncation is negligible in the present experiments. Therefore, both assumptions suggest that the structure of M intermediate may be altered by truncation. PYP_M is in the equilibrium among several substates, whose absorption spectra are different from each other (*14*). Our previous study (*14*) has demonstrated that the spectral shift of M intermediates is coupled with the change in R_g. Unchanged absorption spectra of M intermediates by truncation (Figure 1) (*22*) therefore suggest that the structural change of the main part is not affected by truncation.

In the dark state, Gly7−Leu15 forms a short α-helix which lies parallel to the plane of the β-sheet. The present data can be explained by a model in which residues from Gly7 to Leu15 are detached from the β-sheet upon formation of PYP_M. Surface plasmon resonance experiments have demonstrated that light increases the affinity of PYP to lipid bilayers (*29*). Although PYP is net negatively charged, it can bind to net positively charged, net negatively charged, and electrically neutral bilayers. Therefore, this suggests that the hydrophobic interaction is responsible for this binding. Thus the hydrophobicity of the surface of PYP is increased by light. The short helix at the N-terminal region is likely to be exposed to the solvent and interact with membrane in a hydrophobic manner. In some peripheral proteins, fatty acids covalently bound to the protein act as the anchor. While PYP has no posttranslational modification except for the chromophore, the helix may be the anchor for the membrane or the putative target protein which interacts with PYP_M.

The present experiment demonstrated that the light-induced structural change of PYP is not limited to the N-terminal region. Illumination of T23, which lacks most of the N-terminal loop, caused an increase of R_g by 0.7 Å. However, the Kratky plot demonstrated that the structural change in T23 results in no change in shape. These observations suggest that the main part of PYP globally swells upon photon absorption. The present data did not suggest what kind of structural change causes such a swelling, but molecular

dynamics simulation has suggested that the structures of the loop including Thr50 and that including Met100 are remarkably fluctuated (*30*).

In summary, the structural change for formation of PYP_M is not merely a rearrangement of the surface charge distribution but involves global conformational change, resulting in increases in the dimensions and changes in the shape. This may enable interaction with other molecules such as membrane and proteins. Further detailed information may be obtained by high-resolution structural analysis.

ACKNOWLEDGMENT

The experiments at Photon Factory BL-10C were performed under the approval of the Photon Factory Advisory Committee (Proposal No. 2000G162).

REFERENCES

1. Meyer, T. E. (1985) *Biochim. Biophys. Acta 806*, 175−183.
2. Sprenger, W. W., Hoff, W. D., Armitage, J. P., and Hellingwerf, K. J. (1993) *J. Bacteriol. 175*, 3096−3104.
3. Baca, M., Borgstahl, G. E. O., Boissinot, M., Burke, P. M., Williams, D. R., Slater, K. A., and Getzoff, E. D. (1994) *Biochemistry 33*, 14369−14377.
4. Borgstahl, G. E. O., Williams, D. R., and Getzoff, E. D. (1995) *Biochemistry 34*, 6278−6287.
5. Düx, P., Rubinstenn, G., Vuister, G. W., Boelens, R., Mulder, F. A., Hård, K., Hoff, W. D., Kroon, A. R., Crielaard, W., Hellingwerf, K. J., and Kaptein, R. (1998) *Biochemistry 37*, 12689−12699.
6. Imamoto, Y., Shirahige, Y., Tokunaga, F., Kinoshita, T., Yoshihara, K., and Kataoka, M. (2001) *Biochemistry 40*, 8997−9004.
7. Meyer, T. E., Yakali, E., Cusanovich, M. A., and Tollin, G. (1987) *Biochemistry 26*, 418−423.
8. Hoff, W. D., Van Stokkum, I. H. M., Van Ramesdonk, H. J., Van Brederode, M. E., Brouwer, A. M., Fitch, J. C., Meyer, T. E., Van Grondelle, R., and Hellingwerf, K. J. (1994) *Biophys. J. 67*, 1691−1705.
9. Imamoto, Y., Kataoka, M., and Tokunaga, F. (1996) *Biochemistry 35*, 14047−14053.
10. Ujj, L., Devanathan, S., Meyer, T. E., Cusanovich, M. A., Tollin, G., and Atkinson, G. H. (1998) *Biophys. J. 75*, 406−412.
11. Imamoto, Y., Kataoka, M., Tokunaga, F., Asahi, T., and Masuhara, H. (2001) *Biochemistry 40*, 6047−6052.
12. Imamoto, Y., Mihara, K., Hisatomi, O., Kataoka, M., Tokunaga, F., Bojkova, N., and Yoshihara, K. (1997) *J. Biol. Chem. 272*, 12905−12908.
13. Genick, U. K., Borgstahl, G. E., Ng, K., Ren, Z., Pradervand, C., Burke, P. M., Srajer, V., Teng, T. Y., Schildkamp, W., McRee, D. E., Moffat, K., and Getzoff, E. D. (1997) *Science 275*, 1471−1475.
14. Shimizu, N., Kamikubo, H., Mihara, K., Imamoto, Y., and Kataoka, M. (2002) *J. Biochem. (Tokyo) 132*, 257−263.
15. Lee, B. C., Croonquist, P. A., Sosnick, T. R., and Hoff, W. D. (2001) *J. Biol. Chem. 276*, 20821−20823.
16. Sasaki, J., Kumauchi, M., Hamada, N., Oka, T., and Tokunaga F. (2002) *Biochemistry 41*, 1915−1922.
17. Brudler, R., Rammelsberg, R., Woo, T. T., and Getzoff, E. D. (2001) *Nat. Struct. Biol. 8*, 265−270.
18. Xie, A., Kelemen, L., Hendriks, J., White, B. J., Hellingwerf, K. J., and Hoff, W. D. (2001) *Biochemistry 40*, 1510−1517.
19. Rubinstenn, G., Vuister, G. W., Mulder, F. A., Düx, P. E., Boelens, R., Hellingwerf, K. J., and Kaptein, R. (1998) *Nat. Struct. Biol. 5*, 568−570.
20. Ohishi, S., Shimizu, N., Mihara, K., Imamoto, Y., and Kataoka, M. (2001) *Biochemistry 40*, 2854−2859.
21. Imamoto, Y., Mihara, K., Tokunaga, F., and Kataoka, M. (2001) *Biochemistry 40*, 14336−14343.
22. Harigai, M., Yasuda, S., Imamoto, Y., Yoshihara, K., Tokunaga, F., and Kataoka, M. (2001) *J. Biochem. (Tokyo) 130*, 51−56.
23. Imamoto, Y., Ito, T., Kataoka, M., and Tokunaga, F. (1995) *FEBS Lett. 374*, 157−160.
24. Mihara, K., Hisatomi, O., Imamoto, Y., Kataoka, M., and Tokunaga, F. (1997) *J. Biochem. (Tokyo) 121*, 876−880.
25. Ueki, T., Hiragi, Y., Kataoka, M., Inoko, Y., Amemiya, Y., Izumi, Y., Tagawa, H., and Muroga, Y. (1985) *Biophys. Chem. 23*, 115−124.
26. Svergun, D., Baberato, C., and Koch, M. H. J. (1995) *J. Appl. Crystallogr. 28*, 768−773.
27. Kataoka, M., Nishii, I., Fujisawa, T., Ueki, T., Tokunaga, F., and Goto, Y. (1995) *J. Mol. Biol. 249*, 215−228.
28. Pellequer, J. L., Wager-Smith, K. A., Kay, S. A., and Getzoff, E. D. (1998) *Proc. Natl. Acad. Sci. U.S.A. 95*, 5884−5890.
29. Salamon, Z., Meyer, T. E., and Tollin, G. (1995) *Biophys. J. 68*, 648−654.
30. Shiozawa, M., Yoda, M., Kamiya, N., Asakawa, N., Higo, J., Inoue, Y., and Sakurai, M. (2001) *J. Am. Chem. Soc. 123*, 7445−7446.

BI0264768